Phase space investigation of the lithium amide halides

Rosalind A. Davies [a,b], David R. Hewett [a], Emma Korkiakoski [a], Stephen P. Thompson [c], Paul A. Anderson [a,*]

[a] Hydrogen Storage Chemistry Group, School of Chemistry, University of Birmingham, Edgbaston, Birmingham B15 2TT, United Kingdom
[b] Hydrogen and Fuel Cell Group, School of Chemical Engineering, University of Birmingham, Edgbaston B15 2TT, United Kingdom
[c] Diamond Light Source, Harwell Science and Innovation Campus, Didcot, Oxfordshire OX11 0QX, United Kingdom

ARTICLE INFO

ABSTRACT

An investigation has been carried out into the lower limits of halide incorporation in lithium amide ($LiNH_2$). It was found that the lithium amide iodide $Li_3(NH_2)_2I$ was unable to accommodate any variation in stoichiometry. In contrast, some variation in stoichiometry was accommodated in $Li_7(NH_2)_6Br$, as shown by a decrease in unit cell volume when the bromide content was reduced. The amide chloride $Li_4(NH_2)_3Cl$ was found to adopt either a rhombohedral or a cubic structure depending on the reaction conditions. Reduction in chloride content generally resulted in a mixture of phases, but a new rhombohedral phase with the stoichiometry $Li_7(NH_2)_6Cl$ was observed. In comparison to $LiNH_2$, this new low-chloride phase exhibited similar improved hydrogen desorption properties as $Li_4(NH_2)_3Cl$ but with a much reduced weight penalty through addition of chloride. Attempts to dope lithium amide with fluoride ions have so far proved unsuccessful.

© 2015 Published by Elsevier B.V.

1. Introduction

A large range of materials have been shown to store hydrogen reversibly at a higher density than in its gaseous or liquid form. Mobile applications require the material to be light, causing an increasing focus on the complex hydrides of lighter elements such as aluminium (alanates) [1], boron (borohydrides) [2] and, by analogy, nitrogen (amides) [3,4]. However, despite exhibiting favourable thermodynamics for reversible desorption and absorption of hydrogen, these materials suffer from slow kinetics. Although improvements have been seen on addition of transition metal catalysts [1], this problem is yet to be satisfactorily resolved.

The lithium amide system is one such light metal system that is considered promising for hydrogen storage. Thermal decomposition of $LiNH_2$ alone evolves ammonia rather than hydrogen, but addition of lithium hydride (LiH) creates a pathway that can experimentally produce up to 9.3 wt.% of hydrogen in the two steps shown in Eq. (1) [3]. The second of these requires temperatures above 320 °C and is not generally considered to be a viable hydrogen storage reaction [4]. However, the first stage alone has been shown to release reversibly up to 6.3 wt.% H_2 [3].

$$LiNH_2 + 2LiH \leftrightarrow Li_2NH + LiH + H_2 \leftrightarrow Li_3N + 2H_2 \tag{1}$$
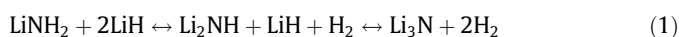
Anderson et al. [5] found that the addition of lithium or magnesium halides to lithium amide results in the formation of new amide halide phases that exhibit not only reduced temperatures of hydrogen release, with little or no release of ammonia, on reaction with LiH or MgH_2, but also increased ionic conductivity relative to $LiNH_2$. However, the addition of heavy halide anions reduces the gravimetric hydrogen capacity of the material. This study investigates the phase space of lithium amide halides with the aim of reducing the gravimetric penalty as much as possible whilst maintaining the observed improvements in the hydrogen storage properties.

2. Materials and methods

Lithium amide (Sigma–Aldrich, 95%) was used without further purification. Anhydrous lithium halides (Sigma–Aldrich, ⩾98%) were dried at 300 °C under high vacuum (1×10^{-6} mbar) for 24 h prior to use. All manipulations were performed in an argon-atmosphere glove box. Amide halides were synthesised by grinding the appropriate halide with $LiNH_2$ in the desired molar ratio, placing the reaction mixture into a quartz tube, and heating under an argon flow (1 bar) at the required temperature for the specified reaction time.

Powder X-ray diffraction (XRD) data were collected on a Bruker D8 Advance diffractometer in transmission geometry with a Cu Kα1 X-ray source. Samples were sealed from the atmosphere between two pieces of amorphous tape. Powder XRD data for structural investigations were collected on a Siemens D5000 diffractometer in capillary mode with a Cu Kα1 X-ray source. Samples were sealed into polyimide capillaries, allowing for long data collection times without degradation. Powder synchrotron X-ray diffraction data were collected on beamline I11 at the Diamond light source, Oxfordshire [6]. Samples were sealed in borosilicate glass capillaries to prevent degradation during transportation and measurement. Powder XRD data

were analysed using the computer program Topas [7], and structure solution was performed through Rietveld refinement of candidate models devised with the help of simulated annealing methods.

Temperature-programmed desorption with mass spectrometry (TPD–MS) data were collected using a home-built TPD apparatus described previously [8], coupled to a quadrupole mass spectrometer (HPR-20, Hiden Analytical). Samples were heated at 2 °C min^{-1} to 400 °C and held at temperature for 1 h before cooling.

3. Results and discussion

3.1. Lithium amide iodide

Lithium amide reacts with lithium iodide at an NH$_2^-$:I$^-$ ratio of 2:1 to form the amide iodide Li$_3$(NH$_2$)$_2$I [5,9]. Rietveld refinement against powder synchrotron XRD data confirmed the structure reported previously [9] of a hexagonal unit cell with a = 7.0650(9) Å, c = 11.521(1) Å.

The reaction, shown in Eq. (2), between lithium amide and lithium iodide was carried out at 150 °C over a range of stoichiometries (0.5 ⩽ z ⩽ 1) for a reaction time of 12 h.

$$(3 - z)\text{LiNH}_2 + z\text{LiI} \rightarrow \text{Li}_3(\text{NH}_2)_{(3-z)}\text{I}_z \qquad (2)$$
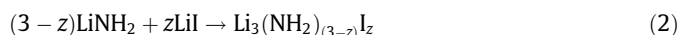
For all the values of z studied, LiNH$_2$ was observed in the XRD patterns alongside the amide iodide. Fig. 1 shows the cell volume of the amide iodide products for values of z between 0.5 and 1. It can be seen that there is, within error, no systematic variation in the cell volume of the amide iodide formed in these reactions. Analysis of the diffraction patterns of the products showed both Li$_3$(NH$_2$)$_2$I and LiNH$_2$ present where the value of z was less than one. The consistency in the lattice parameter and the presence of the starting materials in the products indicate that variations in composition cannot readily be accommodated in this structure.

3.2. Lithium amide bromide

Lithium amide reacts with lithium bromide at an NH$_2^-$:Br$^-$ ratio of 1:1 to form LiNH$_2$Br [5,10], whose low temperature hydrogen desorption mechanism has recently been studied in some detail [11]. At a lower bromide content, it also reacts at a ratio of 6:1 to form Li$_7$(NH$_2$)$_6$Br. Rietveld refinement against powder synchrotron XRD data has confirmed the preliminary structure reported previously for Li$_7$(NH$_2$)$_6$Br [5] of a hexagonal unit cell with a = 9.84893(3) Å, c = 8.9845(3) Å and rhombohedral symmetry.

The limits of the bromide content in the structure were investigated. The reaction between lithium amide and lithium bromide, shown in Eq. (3), was carried out at 250 °C over a range of compositions, between y = 0.6 and 2.33, for a reaction time of 12 h.

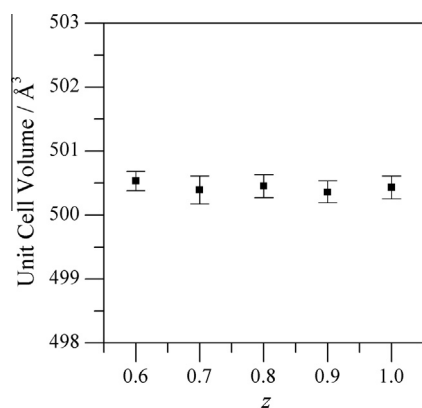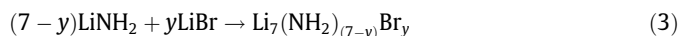$$(7 - y)\text{LiNH}_2 + y\text{LiBr} \rightarrow \text{Li}_7(\text{NH}_2)_{(7-y)}\text{Br}_y \qquad (3)$$

Increasing the bromide level above y = 1 reduced the yield of the amide bromide and large peaks for LiBr were observed in the X-ray diffraction pattern of the product, indicating that the structure cannot accommodate any additional Br$^-$ ions. The product from the reaction at the NH$_2^-$:Br$^-$ ratio 2:1 (y = 2.33) contained mainly unreacted starting materials.

Reducing the bromide content below y = 1 decreased the yield of the amide bromide, with LiNH$_2$ observed in the XRD patterns of the products. A decrease in the cell volume of the amide bromide was observed as y was reduced (Fig. 2), with an overall contraction of 1.24%. However, the presence of LiNH$_2$ in the X-ray diffraction patterns of the products means that it is not possible to calculate the exact extent of the non-stoichiometry directly from the reactant ratios.

3.3. Lithium amide chloride

Lithium amide reacts with lithium chloride at an NH$_2^-$:Cl$^-$ ratio of 3:1, forming Li$_4$(NH$_2$)$_3$Cl [5]. After a reaction time of 1 h a rhombohedral R$\bar{3}$ phase is formed and after 12 h the compound takes a cubic I2$_1$3 form [5]. The reaction shown in Eq. (4) was carried out over a range of compositions between x = 0.5 and 1.75 at 400 °C for both one and 12 h to investigate the effect of composition on the structure of amide chlorides under both kinetic and thermodynamic conditions.

$$(4 - x)\text{LiNH}_2 + x\text{LiCl} \rightarrow \text{Li}_4(\text{NH}_2)_{(4-x)}\text{Cl}_x \qquad (4)$$
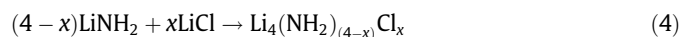
For both reaction times, increasing x above one caused LiCl to be observed in the reaction products, suggesting that no additional Cl$^-$ ions can be accommodated into the structure. For x = 1, as previously observed, reaction for 1 h formed a rhombohedral phase. Decreasing the chloride content caused peak splitting in the X-ray diffraction pattern, which could be refined as a mixture of two rhombohedral phases. The presence of two phases in the product prevents accurate determination of the stoichiometry using the reactant ratios. The unit cell volumes of these two phases are shown in Fig. 3 and show that the two rhombohedral phases have different cell volumes, with the larger likely to be chloride-rich and the smaller chloride-deficient. Decreasing x below 0.7 caused excess LiNH$_2$ to be observed alongside the rhombohedral phases in the diffraction pattern of the product, suggesting that no further decrease in chloride content can be accommodated.

After reaction for 12 h, as described previously [5], a cubic I2$_1$3 phase was observed at x = 1. As the chloride content was reduced, the unit cell volume of this cubic phase decreased (Fig. 4). Decreasing x below 0.75 caused a rhombohedral phase also to be observed in the X-ray diffraction pattern of the product. This new phase was
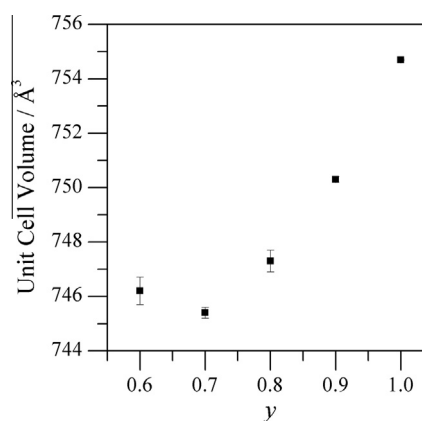

Fig. 1. Unit cell volumes and errors (3σ) for Li$_3$(NH$_2$)$_{(3-z)}$I$_z$.

Fig. 2. Unit cell volumes and errors (3σ) for Li$_7$(NH$_2$)$_{(7-y)}$Br$_y$.